Neuron, Vol. 41, 639–651, February 19, 2004, Copyright ©2004 by Cell Press

Functional Topography of Corticothalamic Feedback Enhances Thalamic Spatial Response Tuning in the Somatosensory Whisker/Barrel System

Simona Temereanca and Daniel J. Simons
Department of Neurobiology
University of Pittsburgh
Pittsburgh, Pennsylvania 15261

Summary

Corticothalamic (CT) projections are ~10 times more numerous than thalamocortical projections, yet their function in sensory processing is poorly understood. In particular, the functional significance of the topographic precision of CT feedback is unknown. We addressed these issues in the rodent somatosensory whisker/barrel system by deflecting individual whiskers and pharmacologically enhancing activity in layer VI of single whisker-related cortical columns. Enhancement of corticothalamic activity in a cortical column facilitated whisker-evoked responses in topographically aligned thalamic barreloid neurons, while activation of an adjacent column weakly suppressed activity at the same thalamic site. Both effects were more pronounced when stimulating the preferred, or principal, whisker than for adjacent whiskers. Thus, facilitation by homologous CT feedback sharpens thalamic receptive field focus, while suppression by nonhomologous feedback diminishes it. Our findings demonstrate that somatosensory cortex can selectively regulate thalamic spatial response tuning by engaging topographically specific excitatory and inhibitory mechanisms in the thalamus.

Introduction

Corticothalamic (CT) feedback is the most prominent anatomical component of thalamocortical circuitry, with CT axons outnumbering thalamocortical (TC) axons by ~10-fold (Guillery, 1967; Liu et al., 1995). Yet its function in sensory information processing remains an unresolved topic of theoretical and experimental interest (see Guillery and Sherman, 2002; Sillito and Jones, 2002). One recent idea advanced in the visual system is that CT feedback enhances object recognition by increasing the firing synchrony of thalamic relay cells that are coactivated by a moving contour (Sillito et al., 1994). An alternate, perhaps related, hypothesis (see Sillito and Jones, 2002) is that cortical feedback increases spatial resolution of thalamocortical inputs by sharpening thalamic receptive field (RF) focus. The latter view is supported by studies in the visual (Murphy and Sillito, 1987) and auditory (Yan and Suga, 1996; Zhang et al., 1997) systems, wherein cortical modulation has been reported at both subthalamic and thalamic levels. In the somatosensory system, a recent study has shown that chronic and acute suppression of activity within the entire hand representation of monkey primary somatosensory cortex leads to an enlargement of hand RFs in the ventroposterior thalamus (Ergenzinger et al., 1998). This raises the possibility that cortical feedback influences thalamic response tuning in the somatosensory system as well, acting via projections to subthalamic or, alternatively, thalamic processing centers.

Experimental evidence supporting these views is limited, as manipulations of cortical activity have led in most studies to modest and inconsistent thalamic effects, consisting of response facilitation, suppression, or both (Yuan et al., 1985; Ghosh et al., 1994; Shin and Chapin, 1990). The variability of the produced effects has been proposed to depend on the topographic correspondence of the studied cortical and thalamic populations (Tsumoto et al., 1978; Yan and Suga, 1996; Zhang et al., 1997). Indeed, an intriguing feature of CT feedback is the precise topographic alignment of TC and CT projections, suggesting that CT connectivity is fundamentally related to its function (see Rouiller and Welker, 2000; Guillery and Sherman, 2002; Murphy et al., 1999). In thalamic nuclei relaying information from ascending pathways, CT influences are mediated by layer VI neurons whose axons contact both excitatory TC cells and, when present, inhibitory interneurons in topographically appropriate regions of the relay nucleus. In addition, CT axons send collaterals to the inhibitory cells of the reticular nucleus (Rt), which receive sensory input from and project back to the thalamic relay nucleus (see Rouiller and Welker, 2000; Deschenes et al., 1998). Conclusions regarding the function of precise CT topography are confounded by experimental manipulations involving widespread cortical removal/suppression or activation and/or by the presence of significant subthalamic processing centers receiving corticofugal projections. In the somatosensory system there is as yet no clear evidence for functional topography of CT effects, and its role in specific modulation of thalamic response tuning is unknown.

Here we address these issues in the rodent somatosensory whisker-to-barrel system. Using their vibrissae, rats are able to perform high-resolution texture discriminations (Carvell and Simons, 1990). Highly spatiotemporally precise information is processed in the thalamic ventral posteromedial nucleus (VPm) by whisker-related groups of neurons called "barreloids" that project to somatotopically corresponding groups of "barrel" neurons in cortical layer IV. Thalamocortical axons also contact dendrites of corticothalamic neurons in the same whisker-related cortical column and receive feedback inputs from them (Hoogland et al., 1987; White and Keller, 1987; Chmielowska et al., 1989; for review see Deschenes et al., 1998). Barreloids are devoid of interneurons, enabling direct assessment of CT effects on TC cell responses. Individual thalamocortical/corticothalamic loops are readily identifiable anatomically and/or electrophysiologically, providing an excellent experimental model for assessing whether and how the spatial focus of thalamic responses depends on the fine-grained topographic organization of the thalamocortical system.

Using reversible pharmacological enhancement of

*Correspondence: temerean@nmr.mgh.harvard.edu

layer VI neuronal activity within a single whisker-related cortical column, we examined CT effects on principal (PW) and adjacent (AW) whisker responses in homologous and adjacent, nonhomologous thalamic barreloids. Sensory-driven CT feedback facilitated responses in homologous thalamic barreloids and suppressed them in nonhomologous barreloids. Both effects were more pronounced for thalamic responses to preferred, or PW, stimulation than nonpreferred, AW, stimulation. These results demonstrate topographic and stimulus-specific CT effects mediated by direct cortical excitation and indirect inhibition through Rt, which selectively enhance or reduce spatial response tuning in TC neurons.

Results

Cortical activity in layer VI, the origin of corticothalamic projections, was enhanced within a small region comprising a single whisker-related column by microiontophoretic application of the GABAa antagonist bicuculline methiodide (BMI). The center of the column was first identified using receptive field mapping by monitoring activity in layer IV. Then, the microiontophoresis electrode was advanced into layer VI as determined using microdrive depth readings and the shape of the stimulus-evoked local field potential (LFP). Along a perpendicular penetration from upper layer V to lower layer VI through a whisker-related column, the LFP changes characteristically in amplitude and time course (Figure 1B), serving as a reliable electrophysiological landmark of the layer V/VI border (e.g., Barth et al., 1989). The location of the microiontophoresis electrode was subsequently confirmed histologically.

BMI application in layer VI reversibly enhances cortical LFP and multiunit (MUA) responses in a dose- and time-dependent fashion (Figures 1C–1F). We evaluated the spatial extent of BMI effects within the cortex by simultaneously recording the activity at the injection site and at sites in layer VI at a distance of $\sim$125 μm and $\sim$250 μm laterally using a second microelectrode (see Figures 1E–1G). BMI application for 20 min at 15 nA gradually increased the LFP and MUA response at the injection site and, at longer latency, 125 μm distant. Drug injection only minimally affected cortical responses at the location 250 μm laterally. Similar distance-dependent effects were observed in the vertical direction. Together, these results indicate that in our conditions BMI injections affect cortical activity within a volume no larger than $\sim$500 microns in diameter, corresponding to the width of a barrel-related cortical column.

Corticothalamic Activation Increases PW Responses in Homologous Thalamic Barreloids

During cortical BMI application, PW-evoked cortical responses were enhanced, as evidenced by increases in LFP amplitude and in MUA magnitude. Concomitantly, LFP and MUA responses in the homologous thalamic barreloid were facilitated. In Figure 2A, for example, an increase in thalamic activity was evident beginning 5.7 ms after LFP response onset and the increase lasted $\sim$12 ms, the period corresponding to the late LFP component. The thalamic multiunit response was transient, occurring within a period of $\sim$30 ms following deflection onset; with cortical BMI application, this response increased by $\sim$65% (Figures 2B and 2C). The enhanced response was followed by a longer, more pronounced decrease in unit firing rate compared to the control response; this decrease is likely mediated by feedback inhibition from Rt. There were no changes in spontaneous activity. The concurrent increases in cortical and thalamic activities during the transient response to whisker deflection indicate that the enhanced thalamic response reflects increased excitatory input from the cortex due to BMI application.

As in the cortex (Figures 1E and 1F), effects of cortical BMI application on thalamic responses were dose and time dependent. Larger iontophoretic currents and longer duration application induced greater increases in thalamic responses in homologous barreloids (Figures 3A and 3B). Large BMI currents could produce uncharacteristically vigorous and long-lasting thalamic responses (e.g., Figure 3A) or occasionally seizure-like activity simultaneously at the cortical ejection site and in the thalamus. To avoid this and in an attempt to produce consistent effects across experiments, we used the smallest ejection currents and the shortest durations of microiontophoresis needed to produce a measurable thalamic effect (see Experimental Procedures).

Increased thalamic responsiveness was observed in 13/16 experiments in which BMI effects were assessed in the homologous thalamic barreloid. In each of these 13 cases, histological reconstructions confirmed that the microiontophoresis electrode was placed in upper/middle layer VI and directly deep to the center or inner edge of the corresponding layer IV barrel. This cortical location contains clusters of barreloid-projecting CT cells (Chmielowska et al., 1989). Data for these 13 cases are summarized in Figure 4. The late component of the thalamic LFP increased, on average, 2.3-fold (Figure 4A), being accompanied by a 1.6-fold average increase in MUA at similar latencies (Figure 4B; paired t test, $p < 0.001$). MUA firing increased significantly in 10/13 individual cases (Student's t test, $p < 0.05$), with no effect in the other three. Effects lasted 10–50 ms and could be observed 3.5–9.5 ms after thalamic response onset and thus 3.0–9.2 ms following the earliest response in the cortex; the timing is consistent with the range of conduction velocities reported for CT neurons in rat (Kelly et al., 2001). Shorter latency increases were clearly observed in the thalamic LFP in 2/13 cases (by 20% and 39%, respectively), but in general such early changes were too small and inconsistent in sign (i.e., either increases or decreases) to be distinguished reliably from noise. Spontaneous MUA activities remained unchanged. In cortex, BMI enhanced PW-evoked LFPs $\sim$2.4-fold (paired t test, $p < 0.001$) and MUA $\sim$1.5-fold ($p < 0.005$). We interpret the findings to mean that BMI application enhanced stimulus-evoked cortical responses, which then, via corticothalamic feedback, facilitated, at slightly longer latency, responses of neurons in the homologous thalamic barreloid.

Interestingly, cortical BMI application failed to affect thalamic activity when the cortical microiontophoresis electrode was located in upper layer V ($n = 2$) or deep to the large septal area between barrel rows C and D ($n =$

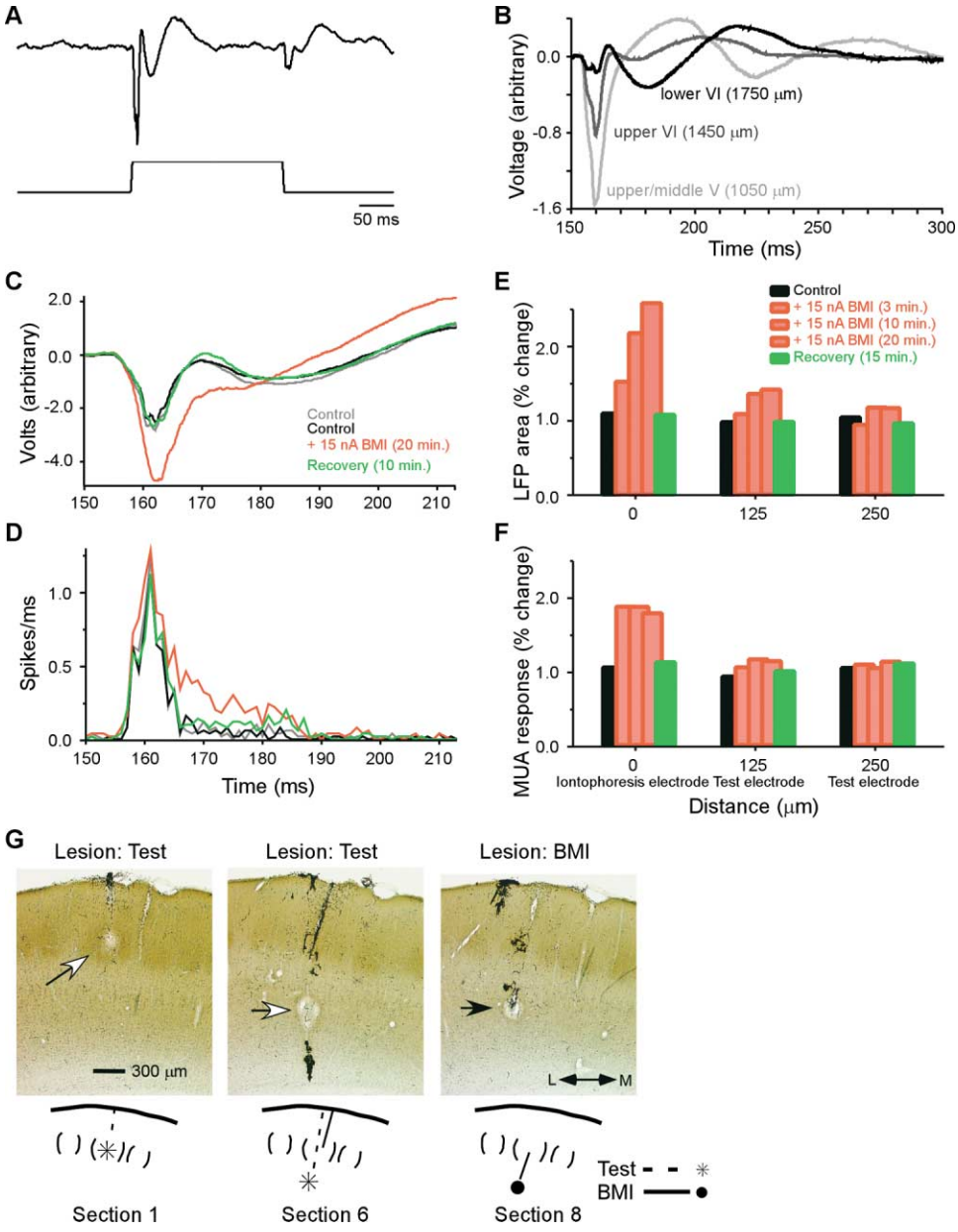

Figure 1. LFP Recordings and BMI Microiontophoresis in Layer VI of Barrel Cortex

(A) Layer VI LFP responses to ramp-and-hold deflections of the column's principal whisker (PW). The LFP signal represents the average of 50 individual trials. Bottom trace represents the stimulus waveform.

(B) The stimulus-evoked cortical LFP is a functional marker of cortical depth. Individual traces show LFP responses to the onset of PW deflection recorded at three different depths along a perpendicular penetration through barrel cortex.

(C and D) Stimulus-evoked layer VI LFPs and MUA are enhanced by microiontophoretic application of BMI. Traces in gray and black show control responses, traces in red show the response after 20 min of BMI ejection, and traces in green show the response 15 min after cessation of BMI application.

(C) Cortical LFP responses.

(D) Cortical MUA responses recorded simultaneously with the LFPs in (C).

(E and F) Spatial extent of BMI effects in layer VI of barrel cortex. A test electrode was placed in layer VI 125 and 250 μm from the BMI electrode, and stimulus-evoked LFPs and MUA were recorded before, during, and after BMI microiontophoresis.

(E) Cortical LFP responses.

(F) Cortical MUA responses recorded simultaneously with the LFPs in (E).

(G) Photomicrographs of 60 μm thick cytochrome-oxidase-stained coronal sections illustrating cortical locations of BMI and test electrodes for data in (E) and (F). Open arrows indicate sites of two electrolytic lesions (layer IV, VI) made in the same track by the test electrode when it was positioned 125 μm from the drug electrode. Filled arrow indicates electrolytic lesion made in layer VI by the BMI electrode. Note that the layer VI lesions are 2 sections apart and the BMI electrode track is oriented slightly anterior-to-posterior and medial-to-lateral. The diagrams on the bottom depict the reconstructed tracks of the microiontophoresis and test electrode.

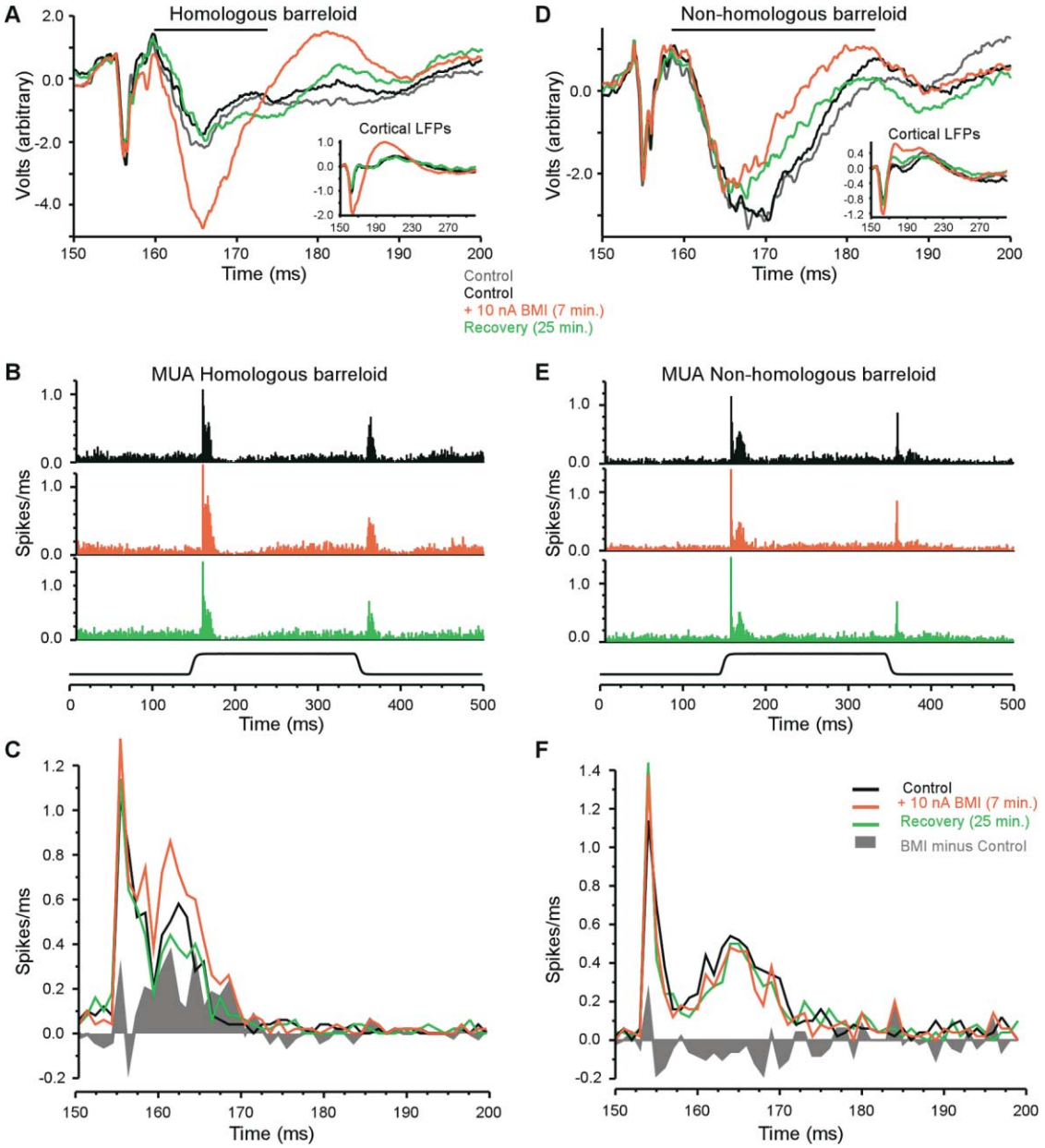

Figure 2. Example of Differential Effects of BMI Microiontophoresis in Layer VI of Barrel Cortex on LFP and MUA Responses to PW Stimulation in Homologous versus Nonhomologous Barreloids

(A) LFP recordings in the D4 barreloid before (gray and black traces), during (red trace), and after (green trace) BMI ejection in layer VI of the D4 barrel-related column. Inset shows simultaneously obtained cortical LFPs. Note changes (indicated by solid bars) in the late component of the LFPs.

(B and C) Simultaneously recorded thalamic MUA in the D4 barreloid. Activity is shown for the total duration of the trial (B) and at an expanded time scale comprising the response to the onset of D4 whisker deflection (C).

(D–F) Data obtained in the D3 barreloid with the same site of cortical BMI application used in (A)–(C). The D3 whisker was deflected. Note enhancement of D4-evoked responses in the D4 barreloid and suppression of D3-evoked responses in the D3 barreloid.

1). Spontaneous and stimulus-evoked thalamic activity remained unchanged in spite of clear increases in cortical activity and in contrast to effects observed in stimulus-evoked responses at the 13 effective cortical sites. The absence of thalamic effects when BMI was ejected at sites slightly displaced from the core location of CT cell bodies is consistent with a small volume of cortical tissue being affected directly by the drug (see Figure 1). Results further indicate that, when observed, cortically induced thalamic effects were mediated by layer VI corticothalamic, and not layer V corticobulbar, neurons (see also below).

Corticothalamic Activation Suppresses PW Responses in Nonhomologous Thalamic Barreloids

Effects of cortical BMI application on PW responses in nonhomologous barreloids were examined in seven

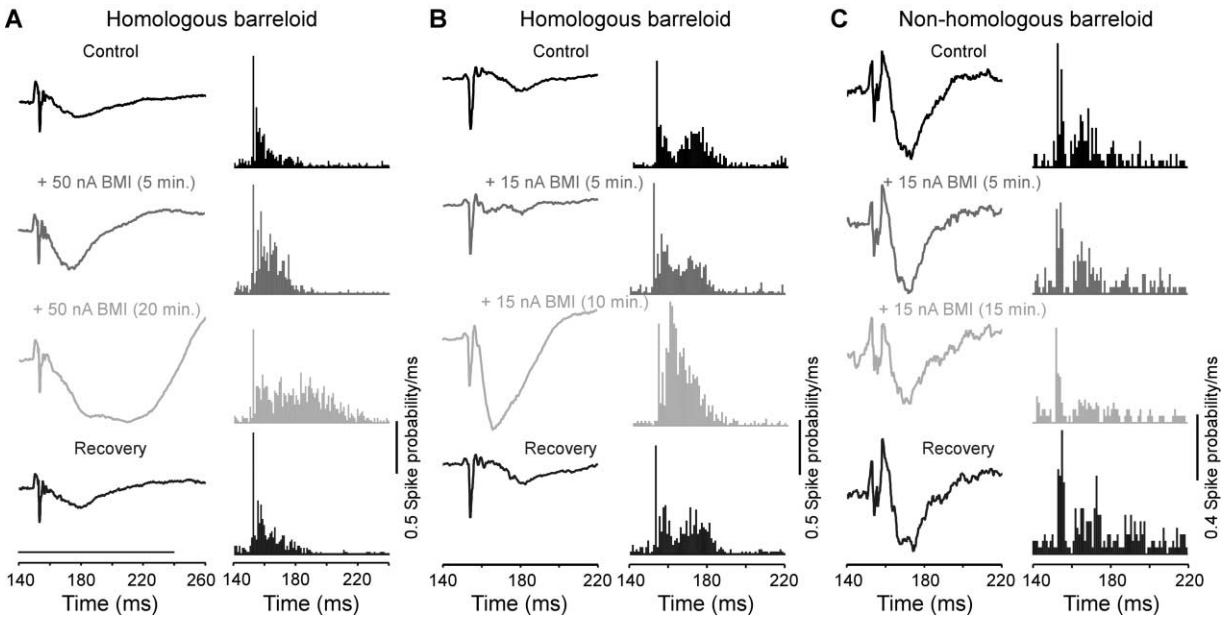

Figure 3. Effects of Cortical BMI Application on Thalamic Responses Are Dose and Time Dependent

Examples of cortical BMI application effects on thalamic PW-evoked responses during long-duration BMI injections with large currents.
(A and B) LFP and MUA responses to deflection onsets recorded in homologous barreloids.
(C) LFP and MUA responses to deflection onsets recorded in a nonhomologous barreloid. Deflections onset occurs at ~145 ms. Longer duration of BMI application and larger iontophoresis currents were associated with larger increases in thalamic responses in homologous barreloids and decreases in nonhomologous barreloids.

experiments; in each case, cortical responses were enhanced and facilitatory effects were observed first in the homologous barreloid. In these seven experiments, the deflected whisker, which is the PW for the thalamic neurons, represents an adjacent whisker (AW) for the cortical neurons at the site of the BMI application. Normally, AW responses (both LFPs and MUA) in the cortex are smaller than PW responses (e.g., insets in Figures 2A and 2D); with BMI, cortical AW LFP responses increased 2.15-fold (paired t test, $p < 0.01$) and MUA 1.81-fold ($p < 0.005$) but remained smaller than BMI-enhanced PW responses. The smaller BMI-induced increases in cortical responses associated with AW deflections did not, however, lead simply to less robust increases in thalamic activity in the neighboring barreloid. Rather, thalamic responses in nonhomologous barreloids were, on average, suppressed (see Figures 2D–2F and 3C), the converse of what was observed in the same experiments when the thalamic recording electrode was in the neighboring, homologous barreloid. Averaged over all seven recording sites, cortical BMI application reduced mean thalamic LFP amplitudes by 15% (Figure 4A) and the simultaneously recorded MUA responses at trend level by a mean 10.3% (Figure 4B; paired t test, $p = 0.098$). For individual recording locations, MUA responses were significantly suppressed in two out of seven cases (Student's t tests, $p < 0.05$) with no effect in the other five (Student's t tests, $p > 0.05$). Again, no consistent changes in spontaneous or plateau activity were observed. Mean changes in both LFPs and MUA responses differed significantly in homologous versus nonhomologous barreloids (Student's t tests, $p < 0.008$). Activity increased in the former and decreased in the latter.

Opposite Effects on Simultaneously Recorded PW Responses in Neighboring Barreloids

The aforementioned LFP and MUA data were obtained using single microelectrodes to sample barreloids sequentially during an experiment, with the homologous barreloid studied first. It is possible that the more varied and weaker effects observed in nonhomologous versus homologous barreloids reflect subtle changes in cortical responsiveness due to multiple BMI applications and/or unanticipated long-term effects in the thalamus. To address this issue, we assessed cortical modulation of simultaneously recorded pairs ($n = 9$) of single thalamic neurons located in immediately neighboring barreloids (i.e., one homologous to the cortical BMI injection site and the other adjacent to it). Opposite effects were observed simultaneously while alternatingly deflecting each neuron's PW. Figures 5A and 5B show PSTHs of two cells' deflection-evoked responses before and after BMI application in the D1 barrel-related column. The cell in the (homologous) D1 barreloid exhibited a significant BMI-induced increase (23%; Student's t test, $p < 0.05$) in its response to deflection of its PW (D1). The simultaneously recorded neuron in the (nonhomologous) D2 barreloid showed no change in activity when its PW (D2) was deflected. Following recovery (data not shown), the microiontophoresis electrode was removed from the D1 barrel-related column and placed in layer VI of the adjacent D2 barrel-related column (Figures 5C and 5D). During BMI injection, the cell in the (now nonhomologous) D1 barreloid exhibited a significant 10.1% decrease (Student's t test, $p < 0.05$) in its D1-evoked response, whereas the response of the cell in the (now homologous) D2 barreloid exhibited a significant 57% increase (Student's t test, $p < 0.05$) to deflections of whisker D2.

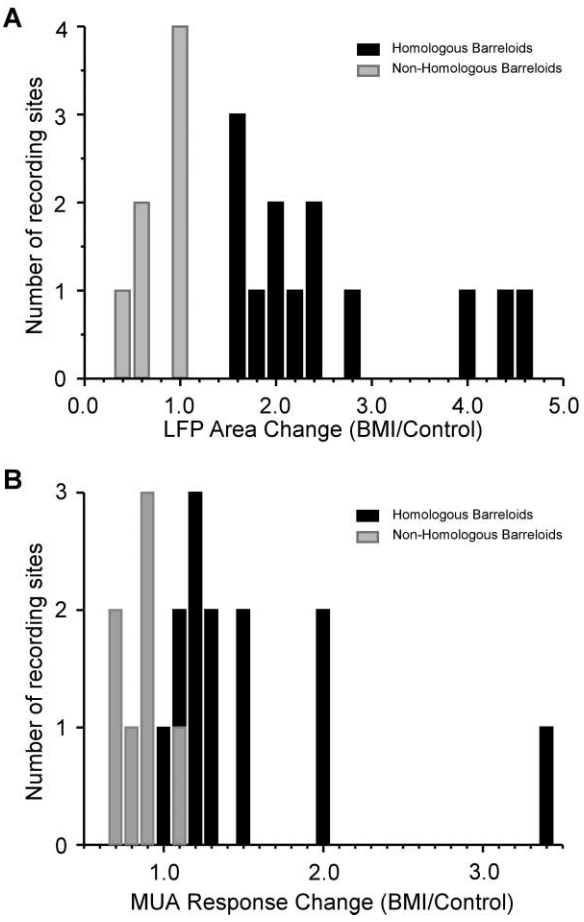

Figure 4. Summary of Effects Induced by Cortical BMI Application on PW-Evoked Thalamic Responses in Homologous and Nonhomologous Barreloids

(A) Effects on thalamic LFP responses (e.g., bars in Figures 2A and 2D).

(B) Effects on thalamic MUA responses to deflection onsets recorded simultaneously with the LFPs in (A). Note that both LFP and MUA responses to PW stimulation were enhanced in homologous barreloids and suppressed in nonhomologous barreloids.

Examination of BMI-induced changes in single-unit responses revealed increases in PW responses in homologous barreloids and concurrent decreases in PW responses in adjacent, nonhomologous barreloids (Figure 6A). In the former, PW responses increased significantly by a mean 18.1% (paired t test, $p < 0.003$), and 5/9 individual cells showed a significant increase in response magnitude (Student's t test, $p < 0.05$), with the remaining showing no change. In nonhomologous barreloids, PW responses decreased significantly, by an average of 10% (paired t test, $p < 0.03$); responses of most individual cells were slightly suppressed, in one case significantly.

Topographically Specific Effects on Response Tuning in Neighboring Barreloids

We assessed the effects of CT feedback on spatial response tuning by examining the relative strengths of PW and AW responses, an indicator of receptive field spatial focus. In addition to the nine simultaneously recorded pairs, we analyzed data from four single units recorded in nonhomologous thalamic barreloids alone, after a (facilitatory) effect of cortical BMI injection had been observed in the homologous barreloid. For these experiments, as above, predrug cortical PW-evoked LFP and MUA responses were larger than AW responses ($p < 0.02$), and this difference persisted during BMI application ($p < 0.02$). Average cortical PW/AW response ratios were similar in control and BMI conditions for both LFPs (2.13 ± 0.48 versus 2.2 ± 0.69, $p > 0.7$) and MUA (1.22 ± 0.31 versus 1.26 ± 0.24, $p > 0.6$). In the thalamus, PW-evoked responses were affected more than AW-evoked responses, and this was the case in both homologous and nonhomologous barreloids (Figure 6B). In homologous barreloids, PW responses increased from 1.65 ± 0.25 spikes/30 ms to 1.95 ± 0.29 spikes/30 ms ($p < 0.003$), whereas AW responses were unaffected ($p > 0.3$). These differential effects yielded a significant increase in PW/AW response ratios from 1.92 ± 0.25 to 2.2 ± 0.23 (Figure 6C; $p < 0.02$). Thus, facilitation by homologous CT feedback increases net response differentials between PW- and AW-evoked activity in the thalamus, enhancing thalamic receptive field focus. In nonhomologous barreloids, on the other hand, PW responses decreased significantly (1.31 ± 0.22 spikes/30 ms versus 1.21 ± 0.21 spikes/30 ms; $p < 0.03$), while AW responses were unaffected ($p > 0.6$). PW/AW response ratios thus decreased from 2.0 ± 0.49 to 1.7 ± 0.4 (Figure 6C, $p < 0.035$). Thus, the response suppression produced by nonhomologous CT feedback has the net effect of reducing the spatial focus of thalamic receptive fields. During enhanced activity in a single cortical column, then, average receptive field focus in neighboring barreloids, equivalent in control conditions, differs by nearly 30% (1.7 versus 2.2).

We investigated possible anisotropies of CT feedback (see Hoogland et al., 1987) by examining whether suppressive effects differed in nonhomologous barreloids depending on their anatomical relationship (within row or within arc) with the homologous barreloid. In total, MUA or single unit responses were obtained in 20 nonhomologous barreloids. In 13 barreloids located within the same whisker-related row as the BMI-injected barrel-related column, PW responses decreased to $92\% \pm 10\%$ of control values, in 4 sites in barreloids situated within the same arc responses decreased to $86\% \pm 22\%$, and in the remaining 3 cases, which were located in a neighboring barreloid one arc and one row removed, the average response was $88\% \pm 6\%$ of control. Thus, suppressive effects appear to be uniform within and across barreloid rows (but see Ghazanfar et al., 2001).

Corticothalamic versus Corticobulbar Effects

We observed corticothalamic effects only when BMI was injected in layer VI. BMI application could, however, enhance activity in nearby layer V, either directly by affecting synapses on their basilar dendrites and/or indirectly by intracolumnar connections involving layer VI cells. Some upper/middle layer V cells project to trigeminal brainstem nuclei, notably the principal sensory nucleus of V, which provides the main afferent input to VPm (see Deschenes et al., 1998). We therefore examined

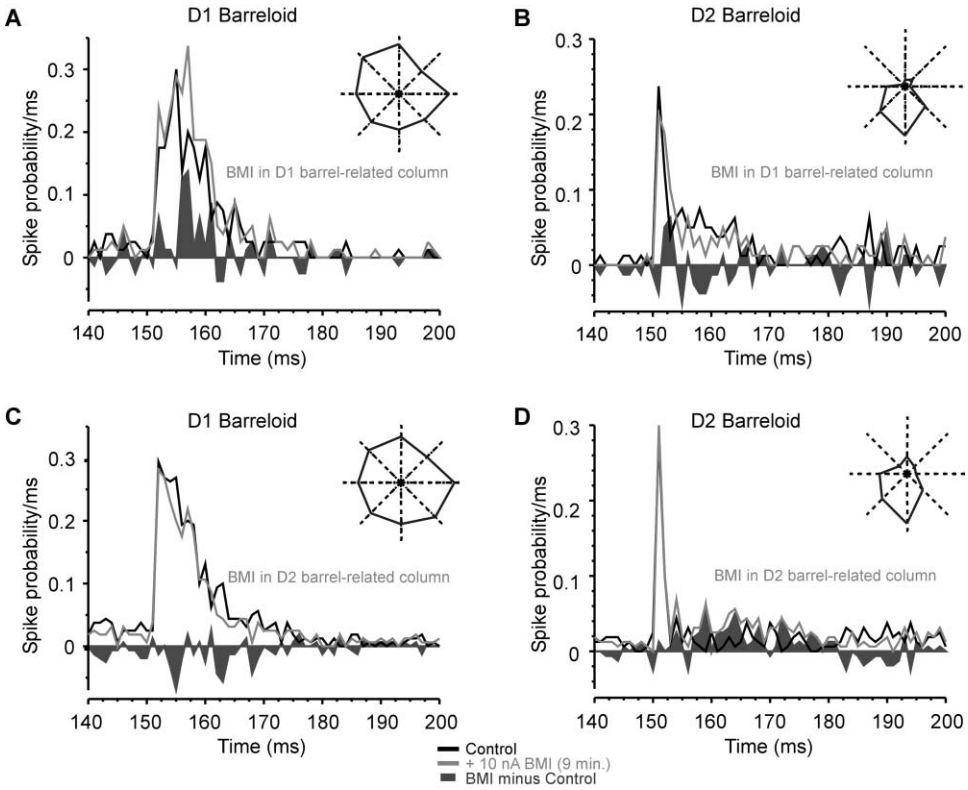

Figure 5. Example of Cortical BMI Effects on Two Neurons Recorded Simultaneously in Adjacent Barreloids

(A and B) PSTHs of each cell's responses to stimulus onsets summed over all eight directions of whisker movement before (black trace) and during (gray trace) BMI ejection in layer VI of the D1 barrel-related column. Shaded area is the difference between the two PSTHs (BMI − Control). Deflections onset occurs at ~145 ms.

(A) Recordings in D1 barreloid.

(B) Recordings in D2 barreloid.

(C and D) PSTHs of thalamic responses recorded from the same cells as in (A) and (B), before and after BMI ejection in layer VI of the D2 barrel-related column.

(C) Recordings in D1 barreloid.

(D) Recordings in D2 barreloid.

Polar plots in each panel show average responses to each of the eight tested deflection directions (all plotted at the same scale). Plots in (A) and (B) were obtained when the BMI electrode was in the D1 barrel-related cortical column; plots in (C) and (D) were obtained after the BMI electrode was placed in the D2 barrel-related column.

specific corticothalamic effects in one experiment by ablating descending fibers at the caudal end of the diencephalon (Figure 7); this manipulation eliminated potential corticobulbar influences. The lesion had no effect on BMI-induced changes in thalamic activity. Both LFP and MUA responses were enhanced in the homologous barreloid and diminished in an adjacent, nonhomologous barreloid (Figures 7B and 7C). Together, results indicate that corticothalamic feedback alone can mediate the differential, highly specific effects reported here in homologous versus nonhomologous thalamic barreloids.

Discussion

Functional Topography of Corticothalamic Projections in the Whisker/Barrel System

Here, we investigated the effects of layer VI corticothalamic feedback on responses in topographically aligned and neighboring thalamic barreloids. Of particular experimental interest was the role of fine-grained anatomical topography in regulating spatial response tuning in thalamocortical circuitry, an issue for which the whisker/barrel system is well suited. We found that effects of sensory-driven CT feedback are highly specific, consisting of enhancement of responses in topographically aligned barreloids and weak suppression in immediately adjacent, nonaligned barreloids. These functional findings are consistent with anatomical studies demonstrating a high degree of reciprocity in the relationship between individual thalamic barreloids and their corresponding barrel-related cortical columns (see Hoogland et al., 1987; Chmielowska et al., 1989; Land et al., 1995; Bourassa et al., 1995; Zhang and Deschenes, 1997; Deschenes et al., 1998; Keller and Carlson, 1999). The functional topography of CT projections reported here in the somatosensory system is similar to that reported previously in the visual system (Tsumoto et al., 1978), as well as that suggested to exist in the auditory system (Yan and Suga, 1996; Zhang et al., 1997; He, 1997, 2003; Zhang and Suga, 2000).

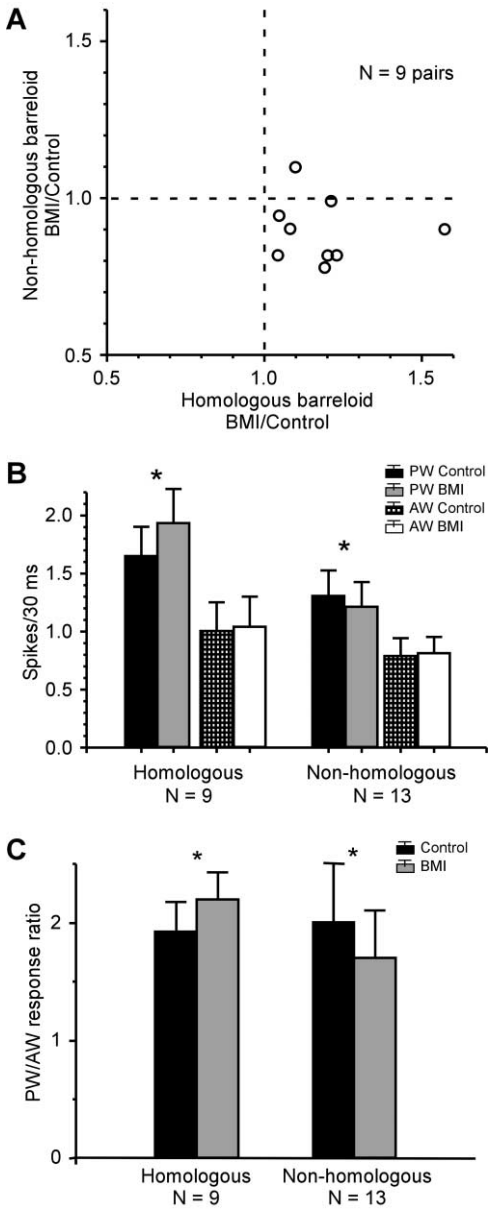

Figure 6. Effects of Cortical BMI Application on Single-Unit Responses from Adjacent Barreloids

(A) Proportional changes in PW responses to deflection onsets in nine pairs of simultaneously recorded cells in two adjacent (i.e., homologous and nonhomologous) barreloids. Note that most data points lie in the quadrant representing increased responses in homologous barreloids and diminished responses in nonhomologous barreloids.

(B) Differential effects of cortical BMI application on PW- and AW-evoked responses in homologous and nonhomologous barreloids. In homologous barreloids, PW-evoked responses increased significantly (asterisk, paired t tests), whereas AW-evoked responses were unchanged. In nonhomologous barreloids, PW-evoked responses were significantly decreased; again, AW-evoked responses were unchanged. Plotted values are mean responses + SEM computed across all deflection angles.

(C) PW/AW response ratios before (black) and during (gray) cortical BMI application in homologous and nonhomologous barreloids. Notice that CT activation significantly enhanced PW/AW response ratios, and thus receptive field focus, in homologous barreloids, while simultaneously decreasing them in nonhomologous barreloids.

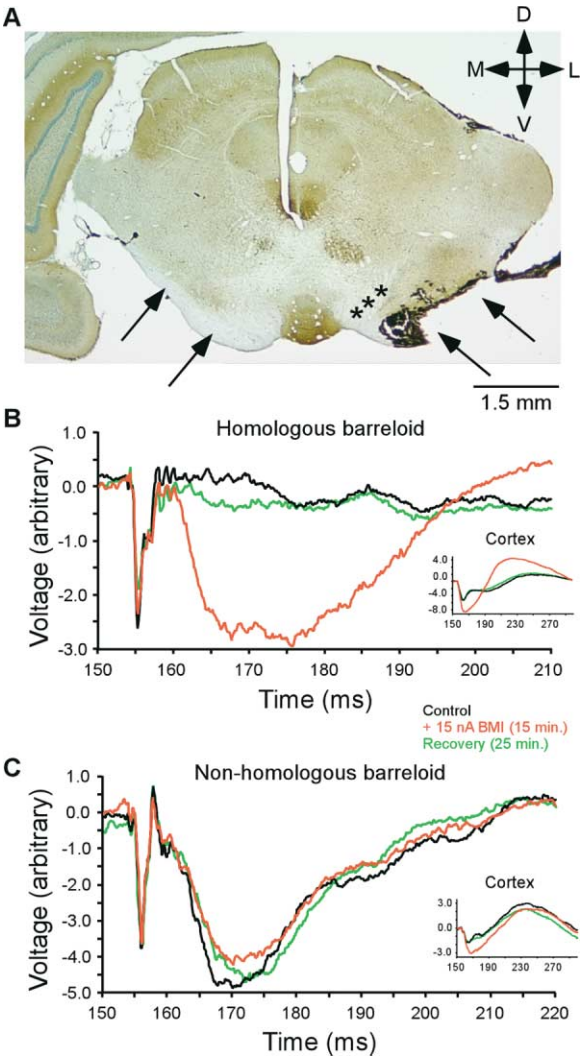

Figure 7. Corticothalamic Effects in the Absence of Corticobulbar Fibers

(A) Lesion of the right cerebral peduncle. Photomicrograph illustrating a cytochrome-oxidase- and Nissl-stained coronal section (60 μm) through the caudal end of the diencephalon. Arrows on the left indicate the intact cerebral peduncle and arrows on the right indicate a lesion of the right cerebral peduncle. Stars indicate the approximate location of the ascending right medial lemniscal fibers.

(B and C) Thalamic LFP recordings in this rat. Cortical BMI application increased PW-evoked LFP responses recorded in the homologous barreloid (B) and decreased PW-evoked responses recorded in an adjacent, nonhomologous barreloid (C). Control traces are illustrated in black, BMI traces in red, and recovery traces in green. Insets in (B) and (C) show cortical LFPs.

We found that CT feedback exerts its effect on spatial response tuning by disproportionately increasing or decreasing thalamic responses in a topographically organized fashion. Activation of a single cortical column enhances PW responses in homologous barreloids and diminishes them in neighboring barreloids. In both cases, AW responses are largely unaffected. The net result is alteration in the relative size of responses to preferred versus nonpreferred stimuli; receptive field focus, a measure of spatial response tuning, is enhanced

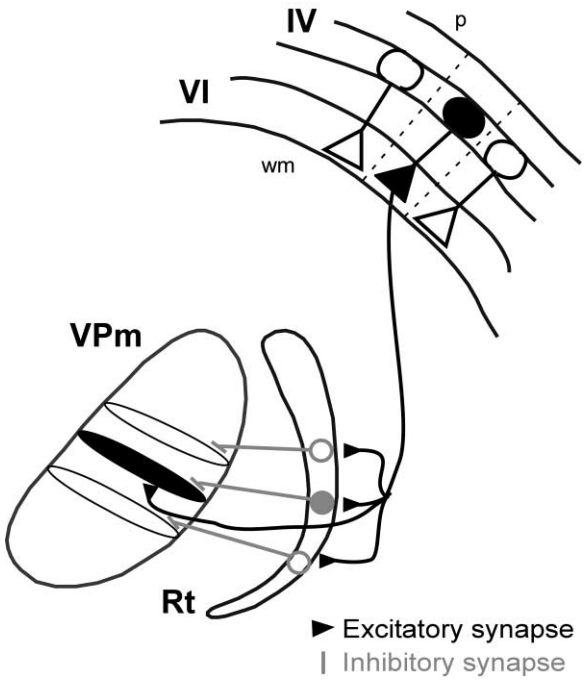

Figure 8. Proposed Model of the Anatomical Relationships among Cortical Barrel-Related Columns, Thalamic Barreloids, and Whisker-Related Modules in the Thalamic Reticular Nucleus

Barrel-related cortical columns are represented by connected triangles (CT cells) and circles (barrel neurons). Barreloids are ovoid-shaped structures in VPm, and inhibitory neurons are located in the laterally displaced Rt. CT cells make excitatory synapses almost exclusively on neurons in the homologous thalamic barreloid and contact Rt neurons associated with several adjacent barreloids; barreloid/RT connections are topographic (Desilets-Roy et al., 2002). The net effect of CT activation is facilitatory in homologous barreloids and suppressive in adjacent, nonhomologous barreloids.

in topographically aligned thalamocortical loops and reduced in adjacent ones. These findings are consistent with an earlier observation in monkey somatosensory system that suppression of cortical activity over a large area encompassing many cortical columns leads to increased thalamic receptive field size and thus a reduction in spatial tuning (Ergenzinger et al., 1998). The present set of experiments differs from previous somatosensory studies in that our cortical manipulations were highly local, restricted to layer VI of a single cortical column. Our findings demonstrate that sensory cortex can selectively regulate thalamic spatial response tuning by acting directly through topographically specific excitatory and inhibitory mechanisms in the thalamus itself (see below). Thalamic effects were observed even after ablation of brainstem-descending fibers, indicating that CT feedback alone can mediate them. Moreover, we found that a critically important experimental variable was the cortical location of the microiontophoresis electrode. Effects were observed when BMI injections were made in upper/middle layer VI, deep to the center or inner edge of the corresponding layer IV barrel. This cortical location contains clusters of barreloid-projecting CT cells (Chmielowska et al., 1989; Kelly et al., 2001).

According to our model (see Figure 8), homologous CT feedback is net excitatory. Cells in the homologous barreloid receive direct excitatory CT inputs and indirect, RT-mediated inhibitory inputs. Direct CT projections to VPm are highly topographic (see Deschenes et al., 1998), as are projections from Rt to VPm (Desilets-Roy et al., 2002). We assume that CT projections to Rt are more topographically diffuse, contacting dendrites of nearby neurons within several whisker-related modules. When the PW is deflected, it produces a large response within its barrel-related cortical column and presumably, in turn, strong feedback facilitation in the homologous barreloid. AW deflections produce smaller responses in the same cortical column and correspondingly weaker facilitation. This would account for our observation that thalamic PW responses were more strongly facilitated than AW responses. The absence of significant AW facilitation may reflect nonlinear integration of weakly efficacious CT inputs on TC cell distal dendrites and proximal inhibitory inputs from Rt (see Peschanski et al., 1983; Rouiller and Welker, 2000). The larger facilitation of PW responses yields an increase in receptive field focus. A net excitatory effect of homologous CT feedback is consistent with findings that cortical inactivation, produced by microiontophoretic application of GABA, diminishes spontaneous firing and renders stimulus-evoked responses shorter (S.H. Lee and D.J.S., unpublished observations), the latter effect being a mirror image of what we observe here.

Nonhomologous CT activation significantly suppresses thalamic PW responses while producing little or no effect on AW responses. The spatial receptive field focus of neurons in nonhomologous barreloids was therefore reduced. Suppression of thalamic PW responses likely reflects the relative absence of direct CT excitatory connections (see Deschenes et al., 1998), permitting any CT-evoked Rt-mediated inhibitory effects to be expressed. These presumably summate with whisker-specific VPm-Rt-VPm inhibition, which is likely to be quite robust (Hartings et al., 2000). The absence of significant AW suppression may reflect, in part, weak AW-evoked VPm-Rt-VPm feedback inhibition (see Simons and Carvell, 1989), which may be only slightly augmented by CT projections to Rt. As in the case of TC cells, afferent (VPm) drive onto RT neurons should be greater than modulatory (CT) influences. Further studies are needed to determine whether our model of response tuning in a single thalamocortical loop would apply when multiple cortical columns are engaged.

Corticothalamic Influences on Sensory Processing in VPm

We observed that CT-mediated enhancement of thalamic activity occurred at latencies of $\geq$3.5 ms (range, 3.5–9.5 ms) relative to the onset of thalamic responses; effects lasted 10–50 ms. No consistent changes were observed in spontaneous activity or in tonic firing during the later phase of the stimulus plateau (see also Yuan et al., 1985, 1986). Thus, pronounced and consistent effects of CT feedback under our experimental conditions were stimulus driven, occurring during transient activation of TC cells by whisker movement (i.e., deflection onset and offset). Corticothalamic fibers contact distal dendrites of TC neurons, where they form gluta-

matergic synapses. Our findings are consistent with CT influences being mediated by both AMPA and NMDA receptors at these synapses (Eaton and Salt, 1996; Kao and Coulter, 1997; Turner and Salt, 1998), which are well suited to mediate faithful, relatively fast transfer of information through thalamus (Castro-Alamancos and Calcagnotto, 2001; see Guillery and Sherman, 2002). The absence of consistent effects on spontaneous and tonic activity make it difficult to evaluate a possible contribution of metabotropic receptors (e.g., McCormick and von Krosigk, 1992; Eaton and Salt, 1996; Godwin et al., 1996; Rivadulla et al., 2002), which are associated with slower, nonspecific changes in TC cell excitability and firing mode. We did find, however, that following cessation of cortical BMI injection, thalamic activity returned to predrug levels more slowly than did cortical activity, suggesting possible long-lasting metabotropic influences.

Previous studies in the visual system have suggested a role for CT projections in enhancing thalamic firing synchrony (Sillito et al., 1994). Feedback-induced effects in the temporal and spatial domain are likely to be functionally related, as sharpening of spatial response tuning could lead to greater precision in the timing of stimulus-driven firing of TC cells (see Sillito and Jones, 2002). In the whisker-to-barrel system, firing synchrony has been proposed to be the salient thalamocortical code, as "preferred" whisker stimuli for cortical barrel neurons are associated with high levels of initial thalamic population activity (i.e., during the first 2–10 ms of the response; Pinto et al., 2000; Temereanca and Simons, 2003). We found that the excitatory effects of CT feedback significantly and consistently enhanced the initial (i.e., 10 ms), though not necessarily earliest, phase of the thalamic response. The period of effective CT enhancement overlaps with the time window for hetero- and homosynaptic facilitation of thalamocortical synapses (i.e., first 8–15 ms; Roy and Alloway, 2001; see Usrey, 2002) and occurs prior to the time of maximal intracortically evoked inhibition (see Pinto et al., 2003).

Experimental manipulations of CT activity have varied widely, employing electrical or pharmacological methods to increase or decrease cortical activity to widely different degrees. Some of the observed effects, notably in somatosensory and auditory systems, may reflect a combination of corticothalamic and corticobulbar effects. Our results, and those from studies of the visual system, clearly indicate specific effects of corticothalamic projections. They also suggest that effects in the thalamus depend on the degree to which cortical activity engages monosynaptic excitatory and disynaptic inhibitory thalamic circuitry. An emerging view, supported by the present findings, is that greater CT activity can lead to increased receptive field tuning in thalamocortical neurons relaying detailed spatiotemporal information from ascending pathways (e.g., in the vibrissa lemniscal system). Available evidence suggests further that CT activation may produce different effects depending on the level and degree of synchronization of cortical activity. For example, under some behavioral conditions, oscillations originating across a widespread cortical region can induce similar periodic firing in thalamic and subthalamic nuclei (Nicolelis et al., 1995). With relatively small and spatially localized increases in cortical excitability, as produced in the present study, the corticothalamic system appears to exert more subtle, modulatory effects, and it does so via stimulus-evoked feedback activity. Cortical feedback may be more likely to affect responses strongly in paralemniscal pathways, where thalamic neurons are less responsive to afferent inputs and more dependent on cortical activity (Diamond et al., 1992; see also Ahissar and Kleinfeld, 2003). Such feedback appears to be mediated by a different population of corticothamic neurons than those thought to have been activated in the present study (Kelly et al., 2001; Rouiller and Welker, 2000; Guillery and Sherman, 2002).

Stimulus-dependent effects of CT feedback might be particularly effective in the presence of ongoing sensory stimulation that occurs during active perceptual-motor behaviors. In the vibrissa somatomotor system, neurons in the deep layers of motor cortex project strongly to layer VI of barrel cortex, providing a potential mechanism for regulating CT activity in a behaviorally dependent fashion. For example, during active whisking, neurons in the vibrissal representation of the motor cortex increase their overall firing rates (Carvell et al., 1996), and such activity could facilitate stimulus-evoked CT activity in whisker/barrel cortex, perhaps analogous to the effects produced here by BMI application. Under these conditions, the enhanced CT response evoked by one whisker perturbation could influence the strength and timing of thalamic responses to immediately following stimuli (Yuan et al., 1985, 1986; Fanselow and Nicolelis, 1999). Our findings indicate that stimulus-evoked responses of CT neurons can contribute to sensory processing by selectively increasing thalamic responses to preferred versus nonpreferred cortical stimuli in a topographically specific fashion. In conjunction with cortical mechanisms for response tuning (see Moore et al., 1999; Pinto et al., 2003), heightened activity in corticothalamic neurons may increase spatial contrast between neighboring whiskers. During ongoing whisker contacts associated with active touch, the high degree of anatomical and functional specificity of stimulus-driven CT feedback could create a core zone of enhanced receptive field focus within the array of thalamic-cortical-thalamic loops.

Experimental Procedures

Surgical Procedures

Adult female albino rats (Sprague-Dawley strain, Hilltop Lab Animals, Scottsdale, PA) were prepared for electrophysiological recordings using surgical procedures described in detail previously (Simons and Carvell, 1989; Temereanca and Simons, 2003). Under halothane anesthesia, the skull was exposed and two small craniotomies, including incising the dura, were made in the right hemisphere overlying the VPm nucleus and barrel cortex. After surgery, halothane was discontinued, and the rat was subsequently maintained in a lightly narcotized state by continuous infusion of fentanyl (Sublimaze, Janssen Pharmaceuticals; $\sim$10 $\mu g \bullet kg^{-1} \bullet h^{-1}$). In order to prevent spontaneous whisker movements, which would prevent use of our whisker stimulators, the animal was immobilized using pancuronium bromide (1.6 $mg \bullet kg^{-1} \bullet h^{-1}$), artificially respired through a tracheal cannula, and kept warm by means of a servo-controlled heating blanket. The condition of the animal was assessed using a computer program that continuously monitored EEG, femoral arterial blood pressure, heart rate, respiration rate, and tracheal airway pressure, all of which remained within normal physiologic ranges throughout the experiments (see Harkness and Wagner, 1989).

Recording Sites

Corticothalamic neurons that project to VPm are clustered below barrel centers and at the layer V/VI border (Chmielowska et al., 1989). Therefore, we placed the microiontophoresis electrode in the middle/upper half of layer VI, as close as possible to the center of the desired barrel-related column. In order to identify the center of a barrel, we oriented the micromanipulator perpendicular to the pial surface and carefully mapped cortical layer IV using stainless steel microelectrodes (1–6 Mohms, Frederick Haer). After a barrel center was identified, the microiontophoresis electrode (see below) was inserted at this location and advanced slowly with a stepping hydraulic microdrive to layer VI using microdrive readings as a preliminary indicator of cortical depth. Electrode depth was adjusted as needed on the basis of the shape of the stimulus-evoked local field potential (see Figure 1B). The homologous thalamic barreloid was then identified using multiunit recordings and the known topography of the thalamic whisker representation.

At the end of the recording session, small electrolytic lesions were made in both thalamus and cortex through the recording microelectrodes. The animal was deeply anesthetized with pentobarbital sodium (Nembutal, 100 mg/kg, i.v.) and perfused transcardially. The brain tissue was subsequently processed for cytochrome oxidase (CO) histochemistry with Nissl counterstain. For cortex, 60 μm frozen serial sections were cut tangential to the pial surface, and sections were used to identify electrode tracks and electrolytic marker lesions. Individual barrels in layer IV, which were easily visualized in CO-stained sections, were used as landmarks for determining histologically the barrel-related column corresponding to the location of the recording/iontophoresis microelectrode. For thalamus, 60 μm sections were cut in a coronal plane and processed as described above. Sections were examined to confirm the location of electrode tracks in VPm. Because of their complex geometry, no attempt was made to identify histologically individual thalamic barreloids.

In one animal, we eliminated possible indirect effects of corticobulbar projections via trigeminal brainstem nuclei (e.g., principal sensory nucleus of V) by making a series of small electrolytic lesions in the crus cerebri near the caudal end of the diencephalon. Lesion sites were targeted at the beginning of the experiment, under halothane anesthesia and prior to neuromuscular blockade, using microstimulation to evoke movements of facial muscles; electrical stimulation at this location antidromically activates corticofugal neurons in layer V of barrel cortex (see Kelly et al., 2001). Lesions were verified histologically (see Figure 7).

Microiontophoresis

We used focal microiontophoretic application of the GABAa antagonist bicuculline methiodide (BMI) to enhance the activity of infragranular cortical neurons. A three-barrel glass microelectrode with a carbon fiber recording channel was used to apply BMI and simultaneously record local field potentials (LFPs) and multiunit activity (MUA). The microelectrodes, assembled using the method reported in Kyriazi et al. (1996), were beveled to tips of 3–8 μm inner diameter. Two of the barrels were filled with 5 mM BMI (Sigma Chemical) in 0.9% NaCl (pH 3.0) and had resistances of 2–12 MOhms. Negative retaining currents of 30–50 nA were used.

Data are reported only from experiments in which BMI application induced clear and reversible increases in cortical activity; failures occurred because of electrode breakage or clogging. MUA and LFPs recorded through the multibarrel microelectrode remained stable during application of retaining current, indicating that there was no significant leakage of the drug. Upon reversal of the current and ejection of BMI, clear effects in the cortex were observed within 5 min (see Figure 1). Preliminary experiments showed that effects of cortical BMI application were dose and time dependent. Longer duration of BMI application and/or larger iontophoresis currents were associated with larger increases in both cortical and thalamic responses (see Figures 1 and 3). Unless otherwise specified, we used the smallest ejection currents needed to produce a measurable thalamic effect and applied BMI for as little time as necessary to record data (10–15 min). Beginning with 5 nA, current injections were increased in 5 nA steps until changes in thalamic activity occurred. If thalamic effects were not observed with the lower current, BMI application was halted for 10 min and then reapplied at the next higher increment, to a maximum of 20 nA in all but one early experiment where 50 nA were used. Currents of 5–15 nA were usually sufficient to induce reversible and reproducible changes in thalamic activity. Data were discarded in the few cases where local seizure-like activity occurred with these longer times/higher currents, typically simultaneously in both cortex and thalamus. We found that, upon cessation of drug application, cortical activity returned to pre-drug levels within 10–20 min, whereas thalamic activity recovered to near-control levels within 30–40 min. We injected BMI no more than 3–6 times during an experiment. Experiments were terminated if cortical or thalamic activity levels did not return to control values following 1 hr of recovery after a drug injection session.

Electrophysiological Recordings

Simultaneous MUA and LFP recordings were obtained in both thalamus and cortex, using low impedance (400 kΩ to 1 MΩ) stainless steel microelectrodes (Frederick Haer, Brunwick, ME) and carbon fiber-loaded glass microiointophoresis/recording microelectrodes (see Temereanca and Simons, 2003). In some experiments, we recorded multiple extracellular single units in thalamus using two quartz-insulated, platinum/tungsten microelectrodes custom-ground to impedances of 6–12 MΩ (Uwe Thomas Recordings, Giessen, Germany). The two electrodes were positioned 100–150 μm apart on the cortical surface and advanced into the brain independently using an Eckhorn microdrive system (Uwe Thomas Recordings). Spike waveforms were parsed online using an amplitude threshold and were saved on disk for more detailed offline analysis using MClust version 2.0 (A. David Redish, University of Minnesota, Minneapolis, MN) to verify the single-unit nature of the recordings (see Bruno and Simons, 2002). Recordings and online data display were performed using custom software written in LABView (National Instruments, Austin, TX).

Vibrissa Stimulation and Experimental Design

Whiskers were deflected using stimulators constructed from piezoelectric bimorphs (Simons, 1983; Pinto et al., 2000). One set of stimuli consisted of caudally directed $\sim$600 μm ramp-and-hold deflections having onset and offset velocities of $\sim$125 mm/s and a plateau duration of 200 ms. Stimulators were attached to the whisker 5 mm from the skin surface, and stimuli were presented at 1.5 s intervals in blocks of 50 trials. In other experiments, whiskers were deflected in eight different directions spanning 360° (in 45° increments) using 1.0 mm ramp-and-hold waveforms having onset and offset velocities of 125 mm/s and 200 ms plateaus; stimulators were attached 10 mm from the base of the hair. Whiskers were deflected randomly in the eight directions, and randomized blocks were delivered 20 times, with interstimulus intervals of 1.5 s. The directional tuning properties of the cells were characterized by constructing polar plots, which show the magnitude of cells' responses to each direction of whisker movement (see insets in Figure 5). The similarities of polar plots recorded several times during a recording session, along with inspection of spike waveforms, were used to verify that the same cells were studied throughout the recording session.

For each recording location, the whisker that evoked the strongest unit response, as determined using an audio monitor and a glass probe to deflect individual whiskers manually, was designated the principal whisker (PW); for cortical recordings/microiontophoresis, the PW was subsequently confirmed anatomically by reference to the overlying layer IV barrel. Immediately neighboring whiskers in the same row or arc were designated adjacent whiskers (AW). In all experiments, cortical activity was monitored using LFPs and MUA activity. Thalamic activity (LFP/MUA or single-unit) was recorded in the homologous barreloid or/and in an immediately adjacent one, usually corresponding to a whisker in the same horizontal row.

Two types of experiments were conducted. In the majority of experiments, thalamic LFPs and MUA recordings were obtained first in the barreloid homologous to the barrel-related column in the cortex, and the PW, which was common to both recording sites, was deflected. Subsequently, the thalamic recording electrode was advanced into an adjacent (nonhomologous) barreloid, and the PW of that barreloid was stimulated. In a second set of experiments, single units were recorded simultaneously in two adjacent bar-

reloids, one of which corresponded topographically with the barrel-related column in which BMI was injected. In this case, two stimulators were separately attached to the PWs corresponding to the recorded barreloids, and stimuli were delivered separately and alternately to the two whiskers.

Data Analysis

The stimulus-evoked cortical and thalamic LFPs are complex waveforms consisting of multiple peaks (Figures 1 and 2). BMI effects on cortical LFP responses were quantified by computing the total area under the curve during the entire duration of the earliest negative component. Thalamic LFP responses to the onset and offset of whisker deflections have an early, fast negativity followed by a slower, late component (Figures 2A and 2D; see also Temereanca and Simons, 2003). As described previously in detail (Temereanca and Simons, 2003), we analyzed separately the first negative wave, or early component, and the slower, second wave, or late component. BMI effects on thalamic LFP responses were quantified by computing (1) the total area under the curve during the entire duration of the early LFP component and (2) the total area under the curve during the period of time corresponding to an increase or decrease in the LFP signal in the case of the late LFP component; effects were presented as ratios of these area measures during BMI application in cortex versus control. Changes in the LFP-evoked response due to uncontrolled changes in the waveform were measured by comparing two pre-BMI files recorded from the same locations. Such signal/"noise" changes were quantified by computing the ratio of the total area under the curve during the entire duration of early and late LFP components, respectively, for the two control files.

Unit responses consisted of transient increases in firing rates to the onset and offset of whisker deflections (Figures 2B and 2E); unit and LFP responses had virtually the same onset latencies. MUA and single-unit responses to the onset and offset of vibrissa deflections were computed as the mean number of spikes recorded for all trials and all directions of movement during different time epochs following deflection onset and offset. When not otherwise specified, response magnitude values reported in the text were computed based on the total 30 ms duration of transient responses to stimulus onset or offset. Spontaneous activity was measured as spike counts during a 100 ms period preceding the stimulus. Parametric statistical tests were used to assess the significance of the effects induced by BMI microiontophoresis in the cortex on cortical and thalamic spontaneous and stimulus-evoked activity.

Acknowledgments

We thank Anissa Myers for histological assistance and Dr. Harold Kyriazi for expert technical assistance and advice throughout. We also thank Drs. Karl Kandler and Deda Gillespie for thoughtful comments on the manuscript. This work was supported by NIH grant NS19950 and NIMH grant MH-61372.

Received: June 18, 2003
Revised: November 6, 2003
Accepted: December 29, 2003
Published: February 18, 2004

References

Ahissar, E., and Kleinfeld, D. (2003). Closed-loop neuronal computations: focus on vibrissa somatosensation in rat. Cereb. Cortex *13*, 53–62.

Barth, D.S., Di, S., and Baumgartner, C. (1989). Laminar cortical interactions during epileptic spikes studied with principal component analysis and physiological modeling. Brain Res. *484*, 13–35.

Bourassa, J., Pinault, D., and Deschenes, M. (1995). Corticothalamic projections from the cortical barrel field to the somatosensory thalamus in rats: a single-fiber study using biocytin as an anterograde tracer. Eur. J. Neurosci. *7*, 19–30.

Bruno, R.M., and Simons, D.J. (2002). Feedforward mechanisms of excitatory and inhibitory cortical receptive fields. J. Neurosci. *22*, 10966–10975.

Carvell, G.E., and Simons, D.J. (1990). Biometric analyses of vibrissal tactile discrimination in the rat. J. Neurosci. *10*, 2638–2648.

Carvell, G.E., Miller, S.A., and Simons, D.J. (1996). The relationship of vibrissal motor cortex unit activity to whisking in the awake rat. Somatosens. Mot. Res. *13*, 115–127.

Castro-Alamancos, M.A., and Calcagnotto, M.E. (2001). High-pass filtering of corticothalamic activity by neuromodulators released in the thalamus during arousal: in vitro and in vivo. J. Neurophysiol. *85*, 1489–1497.

Chmielowska, J., Carvell, G.E., and Simons, D.J. (1989). Spatial organization of thalamocortical and corticothalamic projection systems in the rat SmI barrel cortex. J. Comp. Neurol. *285*, 325–338.

Deschenes, M., Veinante, P., and Zhang, Z.W. (1998). The organization of corticothalamic projections: reciprocity verses parity. Brain Res. Brain Res. Rev. *28*, 286–308.

Desilets-Roy, B., Varga, C., Lavallee, P., and Deschenes, M. (2002). Substrate for cross-talk inhibition between thalamic barreloids. J. Neurosci. *22*, 1–4.

Diamond, M.E., Armstrong-James, M., Budway, M.J., and Ebner, F.F. (1992). Somatic sensory responses in the rostral sector of the posterior group (POm) and in the ventral posterior medial nucleus (VPM) of the rat thalamus: dependence on the barrel field cortex. J. Comp. Neurol. *319*, 66–84.

Eaton, S.A., and Salt, T.E. (1996). Role of N-methyl-D-aspartate and metabotropic glutamate receptors in corticothalamic excitatory postsynaptic potentials in vivo. Neuroscience *73*, 1–5.

Ergenzinger, E.R., Glasier, M.M., Hahm, J.O., and Pons, T.P. (1998). Cortically induced thalamic plasticity in the primate somatosensory system. Nat. Neurosci. *1*, 226–229.

Fanselow, E.E., and Nicolelis, M.A.L. (1999). Behavioral modulation of tactile responses in the rat somatosensory system. J. Neurosci. *19*, 7603–7616.

Ghazanfar, A.A., Krupa, D.J., and Nicolelis, M.A. (2001). Role of cortical feedback in the receptive field structure and nonlinear response properties of somatosensory thalamic neurons. Exp. Brain Res. *141*, 88–100.

Ghosh, S., Murray, G.M., Turman, A.B., and Rowe, M.J. (1994). Corticothalamic influences on transmission of tactile information in the ventroposterolateral thalamus of the cat: effect of reversible inactivation of somatosensory cortical areas I and II. Exp. Brain Res. *100*, 276–286.

Godwin, D.W., Vaughan, J.W., and Sherman, S.M. (1996). Metabotropic glutamate receptors switch visual response mode of lateral geniculate nucleus cells from burst to tonic. J. Neurophysiol. *76*, 1800–1816.

Guillery, R.W. (1967). Patterns of fiber degeneration in the dorsal lateral geniculate nucleus of the cat following lesions in the visual cortex. J. Comp. Neurol. *130*, 197–221.

Guillery, R.W., and Sherman, S.M. (2002). Thalamic relay functions and their role in corticocortical communication: generalizations from the visual system. Neuron *33*, 163–175.

Harkness, J.E., and Wagner, J.E. (1989). The Biology and Medicine of Rabbits and Rodents (Philadelphia, PA: Lea & Febiger).

Hartings, J.A., Temereanca, S., and Simons, D.J. (2000). High responsiveness and direction sensitivity of neurons in the rat thalamic reticular nucleus to vibrissa deflections. J. Neurophysiol. *83*, 2791–2801.

He, J. (1997). Modulatory effects of regional cortical activation on the onset responses of the cat medial geniculate neurons. J. Neurophysiol. *77*, 896–908.

He, J. (2003). Corticofugal modulation of the auditory thalamus. Exp. Brain Res. *153*, 579–590.

Hoogland, P.V., Welker, E., and Van der Loos, H. (1987). Organization of the projections from barrel cortex to thalamus in mice studied with Phaseolus Vulgaris-Leucoagglutinin and HRP. Exp. Brain Res. *68*, 73–87.

Kao, C.Q., and Coulter, D.A. (1997). Physiology and pharmacology of corticothalamic stimulation-evoked responses in rat somatosensory thalamic neurons in vitro. J. Neurophysiol. *77*, 2661–2676.

Keller, A., and Carlson, G.C. (1999). Neonatal whisker clipping alters intracortical, but not thalamocortical projections, in rat barrel cortex. J. Comp. Neurol. *412*, 83–94.

Kelly, M.K., Carvell, G.E., Hartings, J.A., and Simons, D.J. (2001). Axonal conduction properties of antidromically identified neurons in rat barrel cortex. Somatosens. Mot. Res. *18*, 202–210.

Kyriazi, H.T., Carvell, G.E., Brumberg, J.C., and Simons, D.J. (1996). Effects of baclofen and phaclofen on receptive field properties of rat whisker barrel neurons. Brain Res. *712*, 325–328.

Land, P.W., Buffer, S.A., Jr., and Yaskosky, J.D. (1995). Barreloids in adult rat thalamus: three dimensional architecture and relationship to somatosensory cortical barrels. J. Comp. Neurol. *355*, 573–588.

Liu, X.B., Honda, C.N., and Jones, E.G. (1995). Distribution of four types of synapse on physiologically identified relay neurons in the ventral posterior thalamic nucleus of the cat. J. Comp. Neurol. *352*, 69–91.

McCormick, D.A., and von Krosigk, M. (1992). Corticothalamic activation modulates thalamic firing through glutamate "metabotropic" receptors. Proc. Natl. Acad. Sci. USA *89*, 2774–2778.

Moore, C.I., Nelson, S.B., and Sur, M. (1999). Dynamics of neuronal processing in rat somatosensory cortex. Trends Neurosci. *22*, 513–520.

Murphy, P.C., and Sillito, A.M. (1987). Corticofugal feedback influences the generation of length tuning in the visual pathway. Nature *329*, 727–729.

Murphy, P.C., Duckett, S.G., and Sillito, A.M. (1999). Feedback connections to the lateral geniculate nucleus and cortical response properties. Science *286*, 1552–1554.

Nicolelis, M.A., Baccala, L.A., Lin, R.C., and Chapin, J.K. (1995). Sensorimotor encoding by synchronous neural ensemble activity at multiple levels of the somatosensory system. Science *268*, 1353–1358.

Peschanski, M., Ralston, H.J., and Roudier, F. (1983). Reticularis thalami afferents to the ventrobasal complex of the rat thalamus: an electron microscope study. Brain Res. *270*, 325–329.

Pinto, D.J., Brumberg, J.C., and Simons, D.J. (2000). Circuit dynamics and coding strategies in rodent somatosensory cortex. J. Neurophysiol. *83*, 1158–1166.

Pinto, D.J., Hartings, J.A., Brumberg, J.C., and Simons, D.J. (2003). Cortical damping: analysis of thalamocortical response transformations in rodent barrel cortex. Cereb. Cortex *13*, 33–44.

Rivadulla, C., Martinez, L.M., Varela, C., and Cudeiro, J. (2002). Completing the corticofugal loop: a visual role for the corticogeniculate type 1 metabotropic glutamate receptor. J. Neurosci. *22*, 2956–2962.

Rouiller, E.M., and Welker, E. (2000). A comparative analysis of the morphology of corticothalamic projections in mammals. Brain Res. Bull. *53*, 727–741.

Roy, S.A., and Alloway, K.D. (2001). Coincidence detection or temporal integration? What the neurons in somatosensory cortex are doing. J. Neurosci. *21*, 2462–2473.

Shin, H.C., and Chapin, J.K. (1990). Mapping the effects of SI cortex stimulation on somatosensory relay neurons in the rat thalamus: direct responses and afferent modulation. Somatosens. Mot. Res. *7*, 421–434.

Sillito, A.M., and Jones, H.E. (2002). Corticothalamic interactions in the transfer of visual information. Philos. Trans. R. Soc. Lond. B Biol. Sci. *357*, 1739–1752.

Sillito, A.M., Jones, H.E., Gerstein, G.L., and West, D.C. (1994). Feature-linked synchronization of thalamic relay cell firing induced by feedback from the visual cortex. Nature *369*, 479–482.

Simons, D.J. (1983). Multi-whisker stimulation and its effects on vibrissa units in rat SmI barrel cortex. Brain Res. *276*, 178–182.

Simons, D.J., and Carvell, G.E. (1989). Thalamocortical response transformation in the rat vibrissa/barrel system. J. Neurophysiol. *61*, 311–330.

Temereanca, S., and Simons, D.J. (2003). Local field potentials and the encoding of whisker deflections by population firing synchrony in thalamic barreloids. J. Neurophysiol. *89*, 2137–2145.

Tsumoto, T., Creutzfeldt, O.D., and Legendy, C.R. (1978). Functional organization of the corticofugal system from visual cortex to lateral geniculate nucleus in the cat. Exp. Brain Res. *32*, 345–364.

Turner, J.P., and Salt, T.E. (1998). Characterization of sensory and corticothalamic excitatory inputs to rat thalamocortical neurons in vitro. J. Physiol. *510*, 829–843.

Usrey, W.M. (2002). The role of spike timing for thalamocortical processing. Curr. Opin. Neurobiol. *12*, 411–417.

White, E.L., and Keller, A. (1987). Intrinsic circuitry involving the local axon collaterals of corticothalamic projection cells in mouse SmI cortex. J. Comp. Neurol. *262*, 13–26.

Yan, J., and Suga, N. (1996). Corticofugal modulation of time-domain processing of biosonar information in bats. Science *273*, 1100–1103.

Yuan, B., Morrow, T.J., and Casey, K.L. (1985). Responsiveness of ventrobasal thalamic neurons after suppression of SI cortex in the anesthetized rat. J. Neurosci. *5*, 2971–2978.

Yuan, B., Morrow, T.J., and Casey, K.L. (1986). Corticofugal influences of S1 cortex on ventrobasal thalamic neurons in awake rat. J. Neurosci. *6*, 3611–3617.

Zhang, Z.W., and Deschenes, M. (1997). Intracortical axonal projections of lamina VI cells of the primary somatosensory cortex in the rat: a single-cell labeling study. J. Neurosci. *17*, 6365–6379.

Zhang, Y., and Suga, N. (2000). Modulation of responses and frequency tuning of thalamic and collicular neurons by cortical activation in mustached rats. J. Neurophysiol. *84*, 325–333.

Zhang, Y., Suga, N., and Yan, J. (1997). Corticofugal modulation of frequency processing in bat auditory system. Nature *387*, 900–903.